

Ginzburg-Landau analysis of the NJL-model with finite isospinchemical potential

Ginzburg-Landau Analyse des NJL-Modells bei endlichen isospinchemischen Potential

Bachelorarbeit von Dominik Erb

Tag der Einreichung: 26. Januar 2020

1. Gutachten: Priv. Doz. Dr. Michael Buballa

2. Gutachten: Prof. Dr. Guy D. Moore

Darmstadt



TECHNISCHE
UNIVERSITÄT
DARMSTADT

Institute of Nuclear Physics
Nuclei, Hadrons and Quarks
Fachbereich Physik

Abstract

This thesis examines the position of the critical endpoint in the QCD phase diagram for the Nambu-Jona-Lasinio (NJL) model in case of two-flavor quark matter. For this the Ginzburg-Landau analysis will be used on the thermodynamic potential of the NJL-model, which was derived via the mean-field approximation, in the case of chiral limit as well for finite bare quark mass to calculate the position of the critical endpoint to any wanted precision. Special focus lies in the generalization for the case of finite isospinchemical potential. The results will finally be compared to results of past calculations, which were received with other methods, to assess the quality of the new approach.

Zusammenfassung

In dieser Arbeit wird die Lage des kritischen Endpunkts im QCD-Phasendiagramm im Rahmen eines Nambu-Jona-Lasinio (NJL) Modells im Fall von Zwei-Flavor Quark Materie untersucht. Dazu wird auf das aus der Mittelfeldnäherung stammende thermodynamische Potential des NJL-Modells mit Ordnungsparameter M die Ginzburg-Landau Analyse sowohl im chiralem Limes als auch mit endlicher Quarkmasse angewandt, wodurch der kritische Endpunkt beliebig genau bestimmt werden kann. Besonderer Fokus liegt auf der Verallgemeinerung für den Fall von endlichen isospinchemischen Potential. Diese Ergebnisse werden abschließend mit Ergebnissen von vorangegangenen Rechnungen, welche auf anderen Wegen erhalten wurden, verglichen, um Qualität des neuen Ansatzes zu beurteilen.

Inhaltsverzeichnis

1. Introduction	4
2. Quantum Chromodynamics	6
3. Phase transitions	8
4. The Nambu-Jona-Lasinio model	10
4.1. Lagrangian and Symmetries	10
4.2. Finite isospinchemical potential	10
4.3. Mean-field approximation	11
4.4. Regularization method and numeric calculations	14
4.4.1. Regularization	14
4.4.2. Thermodynamic potential and effective mass	15
5. Ginzburg-Landau analysis	21
5.1. General points	21
5.2. Analysis in the chiral limit with no isospinchemical potential	21
5.2.1. The Ginzburg-Landau coefficients	22
5.2.2. Diagram of Ginzburg-Landau coefficients	22
5.3. Analysis in the chiral limit and finite isospinchemical potential	23
5.3.1. Calculation of the Ginzburg-Landau coefficients	23
5.3.2. Conditions for the critical endpoint	24
5.3.3. Diagram of Ginzburg-Landau coefficients	25
5.4. Finite bare mass with no isospinchemical potential	27
5.4.1. The Ginzburg-Landau coefficients	27
5.4.2. Diagram of Ginzburg-Landau coefficients	28
5.5. Finite bare mass and finite isospinchemical potential	29
6. Conclusion and outlook	32
A. Derivatives of the thermodynamic potential	34

1. Introduction

One of the four fundamental forces of nature is the strong interaction. The quantum field theory describing it is called quantum chromodynamics (QCD). This theory explains the interactions between quarks and gluons and was first formulated in the 1970s, after it was discovered, that protons and neutrons are not fundamental particles, but build by quarks. The gluons are the corresponding interaction particles of the theory, similar to the photons in quantum electrodynamics (QED). There exist six flavors of quarks and eight different kinds of gluons. The charge carried by particles interacting with the strong interaction is the so-called color charge. In comparison to the electric charge which has two different kinds of charge, positive and negative, QCD has three different kinds: red, green and blue. This means QCD is a non-abelian gauge theory with symmetry group $SU(3)$. While the photons of QED themselves do not have any electrical charge the gluons do have color charge, which leads to gluon-gluon interactions and makes the theory more complex.

One result of these more complicated interactions is the so-called confinement. This is a property of QCD and describes the fact, that in nature only color neutral particles can be observed. That means quarks and gluons can not exist as free particles, but only in bound states, the color neutral hadrons. On the other hand the gluons and quarks can experience the asymptotic freedom. The coupling constant of QCD vanishes for high energies, hence if the temperature or density is high enough. In this case the hadrons in which the quarks and gluons are confined overlap so much, that they can not be viewed as individual particles anymore. With this the quarks and gluons are not confined like in the low energy case and form the quark-gluon-plasma (QGP). This new state of matter is subject of many experimental investigations and of great importance to understand matter under very high pressure like in neutron stars.

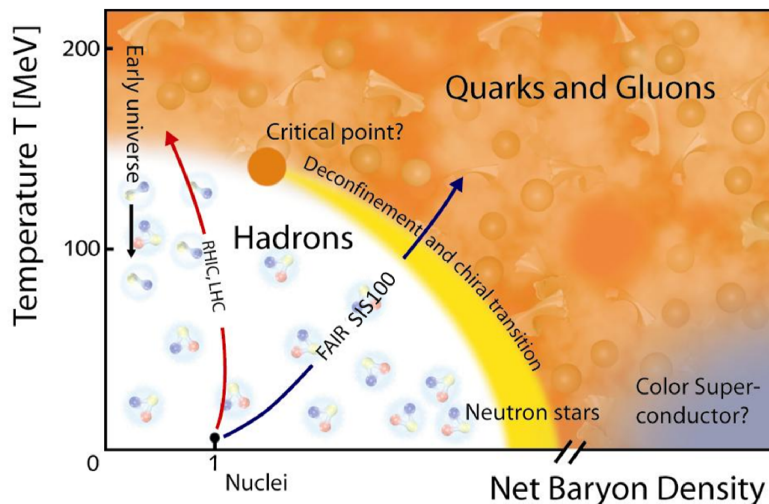


Abbildung 1.1.: Qualitative illustration of the QCD phase diagram taken from [2], including the hadron phase, QGP and a color super conductor phase, as well as the phase boundary between hadrons and QGP with the critical endpoint.

With the hadron phase and the QGP in mind one can create a QCD phase diagram with the temperature and chemical potential represented on the axis. In this diagram the phase transition between the hadron phase and the QGP is of special interest. Investigations in the past have shown, that at low temperatures and high chemical potentials the phase transition between the hadron phase and the QGP is of first order, while at high temperatures and low chemical potentials the transition is of second order. This means that at some point there is a critical endpoint at which there is a change from a first order to a second order phase transition. An example of such a phase diagram can be seen in figure 1.1.

When looking for the critical point one has to differentiate between a phase transition of first order and of second order. Normally one would look at the behavior of the order parameter to make this distinction, but in this case a precise determination of the order of phase transition near the critical point is nearly impossible. Even if the order parameter is continuous in case of second order phase transitions, the first derivative can be discontinuous, which leads to a steep curvature, that can look discontinuous with numerical methods. One method which makes the finding of such critical points much easier is the so-called Ginzburg-Landau analysis, originating from the Ginzburg-Landau theory. With this the determination of the critical point can be transformed to a root finding problem, which is much easier to implement numerically. Such analysis were done in the past with great success.

Until now these Ginzburg-Landau analysis were done with the isospinchemical potential set to zero. This thesis will generalize the methods used to analyze these cases to make the inclusion of a finite isospinchemical potential possible. Finally the results gotten with this generalization will be compared to calculations done in the past, which looked for the critical endpoints via other methods. With this it will be concluded, if such a generalization of the Ginzburg-Landau analysis is feasible.

2. Quantum Chromodynamics

This chapter will give a short overview over the for this thesis relevant parts of QCD before switching to a different and less complex model, which represents these parts very closely, to simplify the calculations. This will be done, because - although it is believed that QCD describes the strong interaction correctly - it is difficult to calculate predictions from the given formulas.

The Lagrangian of the QCD is given by

$$\mathcal{L}_{QCD} = \bar{\psi}(i\cancel{D} - \hat{m})\psi - \frac{1}{4}G_{\mu\nu}^a G_a^{\mu\nu} \quad (2.1)$$

with ψ and $\bar{\psi} = \psi^\dagger \gamma_0$ as the quark fields of six flavors $f = [u, d, s, c, b, t]^T$ and possible color charges $c = [r, g, b]^T$ and $\hat{m} = \text{diag}_f(m_u, m_d, m_s, m_c, m_b, m_t)$ as the mass matrix in flavor space. $G_{\mu\nu}^a$ is the field strength tensor of the gluon field A_μ^a

$$G_{\mu\nu}^a = \partial_\mu A_\nu^a - \partial_\nu A_\mu^a + gf_{abc}A_\mu^b A_\nu^c \quad (2.2)$$

The gluon field is coupled to the quark field by the covariant derivative

$$D_\mu = \partial_\mu - ig \frac{\lambda^a}{2} A_\mu^a \quad (2.3)$$

In the course of this λ_a are the Gell-Mann matrices, which are one possible representation of the infinitesimal generators of the $SU(3)$ symmetry group, f_{abc} is the corresponding structure constant,

$$[\lambda_a, \lambda_b] = 2if_{abc}\lambda_c \quad (2.4)$$

and g is the coupling constant of the QCD.

If one ignores the mass terms, the Lagrangian is invariant under the following transformations:

$$\psi \rightarrow \psi' = e^{i\alpha} \psi \quad (2.5)$$

$$\psi \rightarrow \psi' = e^{i\alpha\lambda_a} \psi \quad (2.6)$$

$$\psi \rightarrow \psi' = e^{i\alpha\gamma_5} \psi \quad (2.7)$$

$$\psi \rightarrow \psi' = e^{i\alpha\lambda_a\gamma_5} \psi \quad (2.8)$$

The symmetry given by 2.5 is a global $U(1)_V$ phase transformation. The corresponding conserved current given by Noether's theorem is the baryon number. The second transformation, 2.6, is only a symmetry transformation, if the masses of the quarks are equal. This is rudimentary true for the up- and down-quark, but false for all other flavors. This transformation is a vector $U(N_f)_V$ transformation where N_f stands for the number of flavors and results in isospin conservation. The third symmetry in 2.7 is an axial $U(1)_A$ transformation and from no further interest. The last transformation, 2.8, is a axial $SU(N_f)_A$ transformation. These transformations do not form a group, but in combination with the other transformations one can get the so-called chiral symmetry. This is an important symmetry which results from the fact, that if the mass terms are zero, no terms in the QCD-Lagrangian mix the right- and left-handed parts of the field given by

$$\psi_{R,L} = \frac{1}{2}(1 \pm \gamma_5)\psi. \quad (2.9)$$

Both of these parts transform independent from another, which gives the following symmetry group:

$$G_{QCD} = SU(N_f)_L \otimes SU(N_f)_R \otimes U(1)_V = SU(N_f)_V \otimes SU(N_f)_A \otimes U(1)_V \quad (2.10)$$

This symmetry is spontaneously broken and results in three Goldstone bosons, the pions. As mentioned before, 2.10 is only for massless quarks a symmetry of QCD, which means in reality, where the mass of the up and down-quarks is finite but very small, the pions are not massless, like real Goldstone bosons, but have some mass. Such bosons are called pseudo-Goldstone bosons.

3. Phase transitions

The best known phases and phase transitions are the three classical states of matter of water, solid, fluid, gas and the transitions between these phases. In general one can speak of a phase transition, if a thermodynamic parameter of a system changes, which results in the change of a so-called order parameter from a non zero state to zero or the other way around. To be more exact the phase goes from a non ordered state to a ordered state, because of a broken symmetry, which results in the emergence of an order parameter. For one given transition there can be one or more order parameters, which can take any possible form, for example they can be scalar or a tensor. Nowadays these phase transitions are classified in transitions of first or second order. If the order parameter behaves not continuous when the phase transition takes place, it is called a first order phase transition, otherwise it is a second order phase transition. Sometimes, when the order parameter does not go exactly to zero, it is called a crossover.

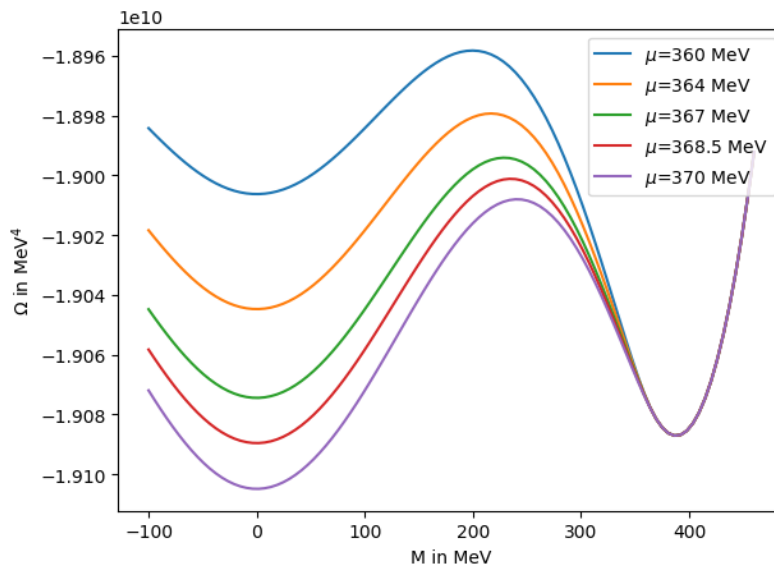


Abbildung 3.1.: Thermodynamic potential of the NJL-model in the chiral limit at $T = 0$ for different chemical potentials when plotted in dependence of the effective quark mass. This shows the case of a first order phase transition, where the thermodynamic potential has multiple minima and the global minimum switches from one minimum to another.

To understand the behavior of the order parameter one can examine the dependence of the thermodynamic potential of this parameter. In figure 3.1 the potential of the Nambu-Jona-Lasinio-model in mean field approximation, which will be induced later, in case of the chiral limit can be seen in dependence of the order parameter, the effective quark mass. The temperature is zero and the chemical potential varies. The different potentials were shifted, such that the minimum at $M \approx 400$ MeV is equal. It is easy to see, how at first the

right minimum is the global minimum, but the difference shrinks when μ gets bigger, until the minimum at $M = 0$ is the new global minimum. When this happens, the first order phase transition takes place.

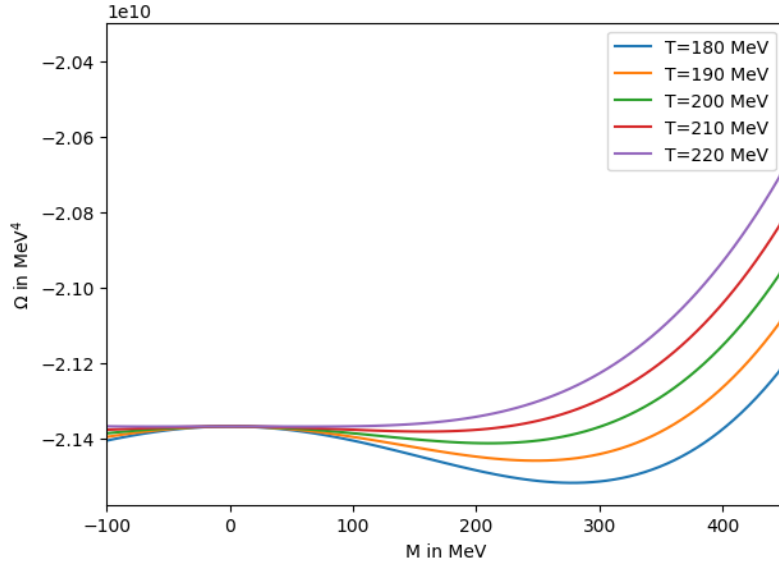


Abbildung 3.2.: Thermodynamic potential of the NJL-model in the chiral limit at $\mu = 0$ for different temperatures when plotted in dependence of the effective quark mass. This shows the case of a second order phase transition, where a minimum slowly merges with another stationary point to form a new global minimum

Conversely figure 3.2 shows how the transition plays out in case of a second order phase transition. In this plot the chemical potential is set to zero and the temperature varies. Again the different thermodynamic potentials were shifted, this time such that they equal at $M = 0$ MeV. In this plot one can see how the right minimum gets less and less deep and wanders to the left side, until it merges with the maximum at $M = 0$ MeV to form the new global minimum.

4. The Nambu-Jona-Lasinio model

The calculations with the QCD-Lagrangian are very complex and in general not very practical. For this reason the Nambu-Jona-Lasinio (NJL) model can be used as a simpler model which represents important properties of the QCD. It was first derived by Y. Nambu and G. Jona-Lasinio in 1961 to describe the interaction of nucleons with nucleons [3] [4], but it was later used to model quark-quark interactions. It was derived before the existence of quarks and the color charge were known, which is why neither the confinement nor the asymptotic freedom are included in the model, but because it represents the chiral symmetry of QCD very well, it was reinterpreted as a low energy effective theory for QCD.

4.1. Lagrangian and Symmetries

For two flavors the Lagrangian of the NJL-Model can be written as follows:

$$\mathcal{L}_{NJL} = \bar{\psi}(i\cancel{D} - \hat{m})\psi + G [(\bar{\psi}\psi)^2 + (\bar{\psi}i\gamma_5\vec{\tau}\psi)^2] \quad (4.1)$$

In this Lagrangian the Dirac spinors do only contain the up- and down-quark in isospin space, $\psi = [u, d]^T$, and \hat{m} is a matrix in the same space with $\hat{m} = \text{diag}(m_u, m_d)$. In the following discussions the mass of the up- and down-quark are assumed to be the same, which is approximately the case, which is why the matrix of the masses will be written without the hat and the indices of the quark masses will be left out, $m = m_u = m_d$. $\vec{\tau}$ represents the Pauli matrices in isospin space.

The Lagrangian is divided into two parts. The first one is the free Dirac field, from which the Dirac equation can be derived. The second part corresponds to four-point interaction between the quarks and consists of a scalar ($\bar{\psi}\psi$) and a pseudoscalar ($\bar{\psi}i\gamma_5\vec{\tau}\psi$) term. More terms can be added to generalize the Lagrangian, which will be discussed later. The factor G represents the coupling constant for the interactions.

The NJL-Lagrangian is invariant under the following transformations, if $m=0$:

$$\psi \rightarrow \psi' = e^{i\alpha}\psi \quad U(1)_V \quad (4.2)$$

$$\psi \rightarrow \psi' = e^{\frac{i}{2}\vec{\theta}\vec{\tau}}\psi \quad SU(2)_V \quad (4.3)$$

$$\psi \rightarrow \psi' = e^{\frac{i}{2}\gamma_5\vec{\theta}\vec{\tau}}\psi \quad SU(2)_A \quad (4.4)$$

with $\vec{\theta} \in \mathbb{R}^3$. On the right side of the transformation it is noted which kind of transformation it is. One can see, that these are the important symmetry transformations of the QCD-Lagrangian as noted in Chapter 2 for the case $N_f = 2$. As it is the case in the QCD-Lagrangian, the transformation in 4.4 is a symmetry transformation only for $m=0$ and 4.3 is a symmetry transformation only if the masses of the quarks are equal.

4.2. Finite isospinchemical potential

The NJL-Lagrangian discussed in section 4.1 holds true, if the up- and down-quark experience the same chemical potential. In general this is not true, which leads to more terms which have to be considered [5]

[6].

$$\mathcal{L}_{NJL} = \mathcal{L}_0 + \mathcal{L}_1 + \mathcal{L}_2 \quad (4.5)$$

The first part, \mathcal{L}_0 , represents the free Dirac field like before

$$\mathcal{L}_0 = \bar{\psi}(i\cancel{\partial} - m)\psi. \quad (4.6)$$

The second and third part describe the interaction and have apart from the scalar and pseudoscalar terms two additional terms, $(\bar{\psi}\vec{\tau}\psi)$ and $\bar{\psi}i\gamma_5\psi$:

$$\mathcal{L}_1 = G_1 [(\bar{\psi}\psi)^2 + (\bar{\psi}\vec{\tau}\psi)^2 + (\bar{\psi}i\gamma_5\psi)^2 + (\bar{\psi}i\gamma_5\vec{\tau}\psi)^2] \quad (4.7)$$

$$\mathcal{L}_2 = G_2 [(\bar{\psi}\psi)^2 - (\bar{\psi}\vec{\tau}\psi)^2 - (\bar{\psi}i\gamma_5\psi)^2 + (\bar{\psi}i\gamma_5\vec{\tau}\psi)^2] \quad (4.8)$$

The symmetry transformations in section 4.1 still hold true under the given assumptions and if one considers the limit case $G_1 = G_2$, it is easy to see, that the Lagrangian is equal to the Lagrangian discussed before. To represent this fact the coupling constants will be set in the following way:

$$G_1 = (1 - \kappa) \cdot G \text{ and } G_2 = \kappa \cdot G \quad (4.9)$$

The parameter κ is restricted to the interval $[0, \frac{1}{2}]$ with the border case $\kappa = \frac{1}{2}$ representing the situation discussed before. Later it will be shortly mentioned, how the get the Lagrangian in 4.1 from the more general Lagrangian, if the quarks experience the same chemical potential.

4.3. Mean-field approximation

For calculation purposes it is advantageous to have the thermodynamic potential of a system. To get this potential from the Lagrangian one has to linearize the latter, which can be done via the mean-field approximation. In this approximation only small deviations from the expected value are considered. For example if one considers the scalar term of the interactions it can be written as

$$\bar{\psi}\psi = \langle \bar{\psi}\psi \rangle + \delta(\bar{\psi}\psi) \quad (4.10)$$

where $\langle \bar{\psi}\psi \rangle$ is the mean value and $\delta(\bar{\psi}\psi)$ is a very small deviation of the mean value. This means the quadratic term can be approximated by

$$(\bar{\psi}\psi)^2 \approx \langle \bar{\psi}\psi \rangle^2 + 2\langle \bar{\psi}\psi \rangle \delta(\bar{\psi}\psi) \quad (4.11)$$

by leaving out the quadratic term of $\delta(\bar{\psi}\psi)$. By using the definition of $\delta(\bar{\psi}\psi)$ equation 4.11 can be written as

$$(\bar{\psi}\psi)^2 \approx 2\langle \bar{\psi}\psi \rangle (\bar{\psi}\psi) - \langle \bar{\psi}\psi \rangle^2. \quad (4.12)$$

The same approach can be done with all other terms. Lastly in this thesis only the following mean values will be considered, the quark condensates, which will be given a new name for overview purposes, by setting the other ones to zero:

$$\sigma_u := \langle \bar{u}u \rangle \quad (4.13)$$

$$\sigma_d := \langle \bar{d}d \rangle \quad (4.14)$$

In this definition u and d represent the field of the up- and down-quark.

The Lagrangian written as a function of these fields takes the following form:

$$\begin{aligned} \mathcal{L}_{NJL} = & \bar{u}(i\cancel{\partial} - m)u + \bar{d}(i\cancel{\partial} - m)d \\ & + 2G_1[(\bar{u}u)^2 + (\bar{d}d)^2 + 2(\bar{u}d)(\bar{d}u) + (\bar{u}i\gamma_5u)^2 + (\bar{d}i\gamma_5d)^2 + 2(\bar{u}i\gamma_5d)(\bar{d}i\gamma_5u)] \\ & + 4G_2[(\bar{u}u)(\bar{d}d) - (\bar{u}d)(\bar{d}u) - (\bar{u}i\gamma_5u)(\bar{d}i\gamma_5d) + (\bar{u}i\gamma_5d)(\bar{d}i\gamma_5u)] \end{aligned} \quad (4.15)$$

With the mean-field approximation and the noted definitions this Lagrangian can be simplified to

$$\begin{aligned}\mathcal{L}_{MF} = & \bar{u}(i\cancel{\partial} - m + 4G_1\sigma_u + 4G_2\sigma_d)u \\ & + \bar{d}(i\cancel{\partial} - m + 4G_1\sigma_d + 4G_2\sigma_u)d \\ & - 2G_1(\sigma_u^2 + \sigma_d^2) - 4G_2\sigma_u\sigma_d\end{aligned}\quad (4.16)$$

By sorting the terms in this way it is easy to see that this formulation is equivalent to the Lagrangian of two fermions with masses M_u and M_d given by

$$M_u = m - 4G_1\sigma_u - 4G_2\sigma_d \quad (4.17)$$

$$M_d = m - 4G_1\sigma_d - 4G_2\sigma_u \quad (4.18)$$

These new masses are called effective quark masses or constituent quark masses and this set of equations is called the gap equations. The emergence of these new masses can be explained by the quark self energy. Consider the propagation of a single quark. This quark can in fact interact with itself. The propagator which includes all the possible self interactions is called the dressed propagator, while the propagator that does not include the self interaction terms is called bare propagator. The dressed propagator can be understood as a kind of geometric series of bare propagators with an incising number of self-energy vertices. In equation form it can be written as follows:

$$iS(p) = iS_0(p) + iS_0(p)(-i\Sigma)iS_0(p) + iS_0(p)(-i\Sigma)iS_0(p)(-i\Sigma)iS_0(p) + \dots \quad (4.19)$$

Where $S(p)$ denotes the dressed propagator, $S_0(p)$ the bare propagator and Σ the self-energy operator. This equation can be shortend in the following way:

$$iS(p) = iS_0(p) + iS_0(p)(-i\Sigma)iS(p) \quad (4.20)$$

This equation in form of Feynman diagrams can be seen in figure 4.1. By multiplying the equation with the



Abbildung 4.1.: Gap equation in form of Feynman diagrams taken from [8]. The drawn through lines represent the dressed propagators, while the dashed line represent the bare propagators.

inverse propagators from left and right, one can get

$$S_0^{-1}(p) = S^{-1}(p) + \Sigma. \quad (4.21)$$

With the expression $S^{-1}(p) = \cancel{\not{p}} - m$ this leads to

$$\cancel{\not{p}} - m = \cancel{\not{p}} - M + \Sigma \quad (4.22)$$

$$\Rightarrow M = m + \Sigma \quad (4.23)$$

This equation is another way of writing equation 4.17 and 4.18. It leads to gap of $\Delta E = 2M$ in the quark spectrum, which is the reason it is called the gap equation. With the effective quark masses the Lagrangian in 4.16 can be written as

$$\mathcal{L}_{MF} = \bar{u}(i\cancel{\partial} - M_u)u + \bar{d}(i\cancel{\partial} - M_d)d - 2G_1(\sigma_u^2 + \sigma_d^2) - 4G_2\sigma_u\sigma_d \quad (4.24)$$

This formulation consists of two free fermions and other terms, which do not depend on the fields. Therefore the Hamiltonian can now be written as

$$\mathcal{H}_{MF} = \mathcal{H}_0(M_u) + \mathcal{H}_0(M_d) + 2G_1(\sigma_u^2 + \sigma_d^2) + 4G_2\sigma_u\sigma_d \quad (4.25)$$

where \mathcal{H}_0 is the one-particle Hamiltonian.

One can now get the thermodynamical potential Ω as the sum of the thermodynamic potential of two free fermions and terms which do not depend on the fields.

$$\Omega_{MF} = \Omega_0(M_u, T, \mu_u) + \Omega_0(M_d, T, \mu_d) + 2G_1(\sigma_u^2 + \sigma_d^2) + 4G_2\sigma_u\sigma_d \quad (4.26)$$

As noted the two fermions do not experience the same chemical potential. In the following μ represents the mean chemical potential, μ_u the chemical potential of the up-quark and μ_d the chemical potential of the down-quark. The difference between the experienced potential of both quarks is called the isospinchemical potential μ_I . For convenience purposes the difference between μ_u or μ_d respectively and the mean value μ can be introduced

$$\Delta\mu := \frac{1}{2}\mu_I = \frac{1}{2}|\mu_u - \mu_d| \quad (4.27)$$

which leads to:

$$\mu_u = \mu + \Delta\mu \quad (4.28)$$

$$\mu_d = \mu - \Delta\mu \quad (4.29)$$

The thermodynamic potential of the free part is given by

$$\Omega_0(M, T, \mu) = -2N_C \int \frac{d^3\vec{p}}{(2\pi)^3} \left[E_{\vec{p}} + T \ln(1 + \exp(-\frac{1}{T}(E_{\vec{p}} - \mu))) + T \ln(1 + \exp(-\frac{1}{T}(E_{\vec{p}} + \mu))) \right] \quad (4.30)$$

In the course of this N_C is the number of colors, T is the temperature, μ the chemical potential and $E_{\vec{p}} = \sqrt{\vec{p}^2 + M^2}$ is the energy of the particle. With equations 4.17 and 4.18 the thermodynamic potential can be interpreted as a function of σ_u and σ_d . A physical system will always tend to be in a thermodynamic equilibrium. This is the case, if the thermodynamic potential has an minimum or maximum. The equilibrium is stable, if the system is in the global minimum of the thermodynamic potential. The minima and maxima points can be calculated by taking the gradient of the thermodynamic potential and set it to zero. By doing this one can get the following requirement for the mean values:

$$\sigma_f = -2N_C \int \frac{d^3\vec{p}}{(2\pi)^3} \frac{M_f}{E_{\vec{p}}} (1 - n_{\vec{p},f} - \bar{n}_{\vec{p},f}) \quad (4.31)$$

These equations have to be solved self consistent together with equation 4.17 and equation 4.18. To simplify the equation the Fermi-Dirac-statistics are used:

$$n_{\vec{p},f} = \frac{1}{1 + \exp(\frac{1}{T}(E_{\vec{p}} - \mu))} \quad (4.32)$$

$$\bar{n}_{\vec{p},f} = \frac{1}{1 + \exp(\frac{1}{T}(E_{\vec{p}} + \mu))} \quad (4.33)$$

In the case of $\Delta\mu = 0$ the thermodynamic potential takes the following form:

$$\Omega_{\Delta\mu=0} = 2\Omega_0(M, T, \mu) + \frac{(m - M)^2}{4G} \quad (4.34)$$

This is because as a result of $\Delta\mu$ being equal to zero, σ_u and σ_d always have the same value, which simplifies the equations. Additionally equation 4.34 does in no way depend on κ . From this one can conclude, that the Lagrangian does not depend on the value of κ , which means $\kappa = \frac{1}{2}$ can be chosen. This simplifies the more general Lagrangian of equation 4.5 to the Lagrangian of equation 4.1

4.4. Regularization method and numeric calculations

4.4.1. Regularization

Interactions in the NJL-model happen by four-point interactions. Hence the theory cannot be renormalized, which leads to occurrences of divergent integrals, some of which are seen in the section beforehand. These integrals have to be regularized by some method. This thesis uses for this a simple $\mathcal{O}(3)$ -cutoff. This means the divergent integrals are evaluated up to a cutoff Λ . This kind of regularization is very easy to implement and leads to faster calculations, sometimes even to analytical solutions for the integrals, but like all regularization methods it has some problems. The most obvious of which is the loss of invariance under Poincaré-transformations of the integral. For the calculations in this thesis this invariance is not as important as the problems of other regularization methods, because the rest frame of the medium is preferred over other frame of references; there is no reason to change the frame of reference.

With the selection of the regularization method one has to fix the free parameters of the model. For this thesis the following parameters are used:

$$m = 5.6 \text{ MeV} \tag{4.35}$$

$$\Lambda = 587.9 \text{ MeV} \tag{4.36}$$

$$G\Lambda^2 = 2.44 \tag{4.37}$$

This parameters originate from [7] where they were determined by fitting them to proper values for the pion mass $m_\pi = 135 \text{ MeV}$, the pion decay constant $f_\pi = 92.4 \text{ MeV}$ and the quark condensate $\langle \bar{\psi}\psi \rangle^{1/3} = -240.8 \text{ MeV}$ in the vacuum. As an realistic value for the isospinchemical potential $\Delta\mu = 30 \text{ MeV}$ was chosen [10]. Later on some calculations will be done with slightly different parameters. The reason for this is to get comparability to calculations done in the past [10]. These parameters are as follows:

$$m = 6 \text{ MeV} \tag{4.38}$$

$$\Lambda = 590 \text{ MeV} \tag{4.39}$$

$$G\Lambda^2 = 2.435 \tag{4.40}$$

With the necessary parameters set the thermodynamic potential can now be calculated. To show how the potential and the effective mass behave under various circumstances, $\Delta\mu$ will first be set to zero. The reason for this is, because a plot of the potential with finite $\Delta\mu$ is necessarily three dimensional, which makes it harder to see elementary properties of the potential.

4.4.2. Thermodynamic potential and effective mass

Zero isospinchemical potential

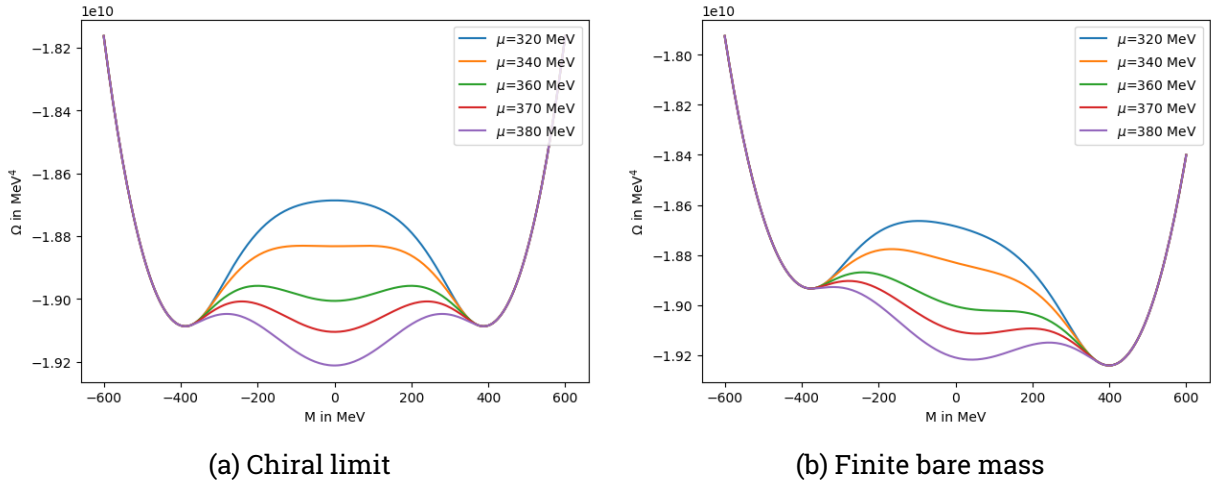
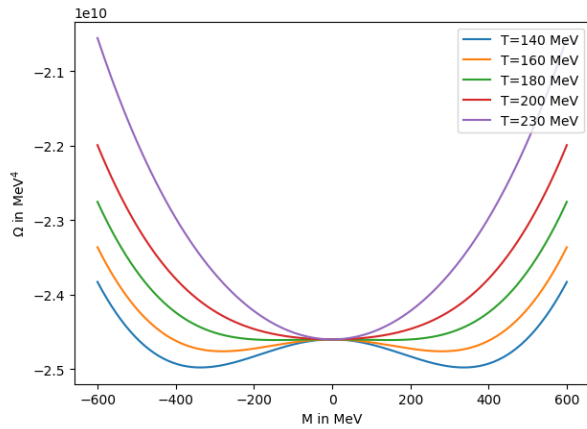


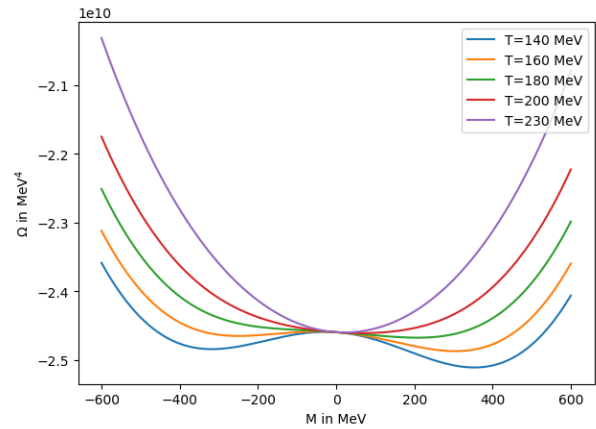
Abbildung 4.2.: Thermodynamic potential of the NJL-model in dependence of the order parameter M at temperature $T = 0$ for different chemical potentials. The potentials were shifted in such a way, that the minima at $M \approx 400$ MeV are equal. A first order phase transition can be seen in both cases.

Figure 4.2 shows different forms of the thermodynamic potential with varying values of μ at $T = 0$. Going along the μ -axis of the phase diagram like this, a first order phase transition happens. This can be seen in the chiral limit in figure 4.2a as well as with finite bare mass in figure 4.2b. The potential at first has three stationary points, two of which are minima. In the chiral limit these minima are degenerate, while with finite bare mass the minimum at positive values for M is preferred. When μ gets bigger, in total five stationary points can be seen with a new minimum in the middle. If μ is big enough this becomes the new global minimum. At that chemical potential the first order phase transition happens. Another property at the thermodynamic potential in the chiral limit can be clearly seen in figure 4.2a. In the chiral limit the potential is an even function, which means it is symmetric around zero. This will be a common theme for all later figures.

Figure 4.3 shows the opposite case of what happens, if one would set the chemical potential to $\mu = 0$ and vary the temperature. Similar as described above the thermodynamic potential shows three stationary points at first with two minima. But this time as one goes along the T -axis these minima wander to the middle with the difference between the minima and the maximum in the middle getting smaller and smaller, until all stationary points merge together to form one global minimum. In this case a second order phase transition happens. To make the comparison between the different forms of the potential easier, the potentials were shifted in such a way, that they equal at $M = 0$.



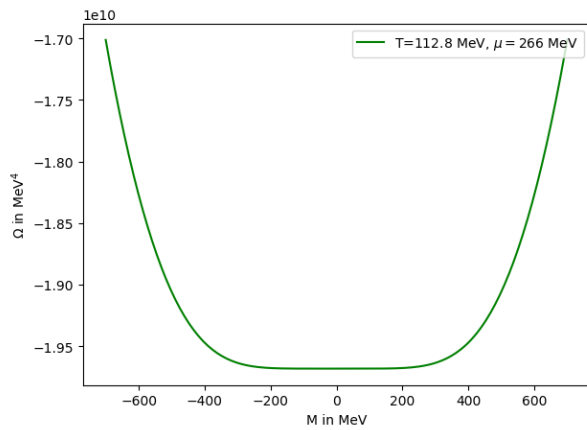
(a) Chiral limit



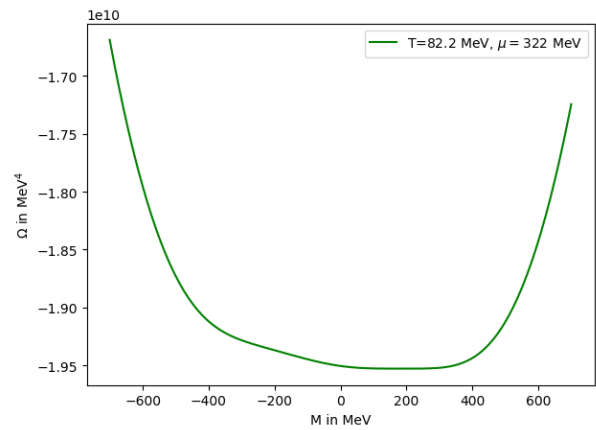
(b) Finite bare mass

Abbildung 4.3.: Thermodynamic potential of the NJL-model in dependence of the order parameter M at $\mu = 0$ for different temperatures. The potentials were shifted in such a way, that they are equal at $M = 0$. A second order phase transition can be seen.

The form of the thermodynamic potential at the critical endpoint combines the features of the first two cases as seen in figure 4.4. The result of this is a flat curve over a relatively long interval around $M = 0$.

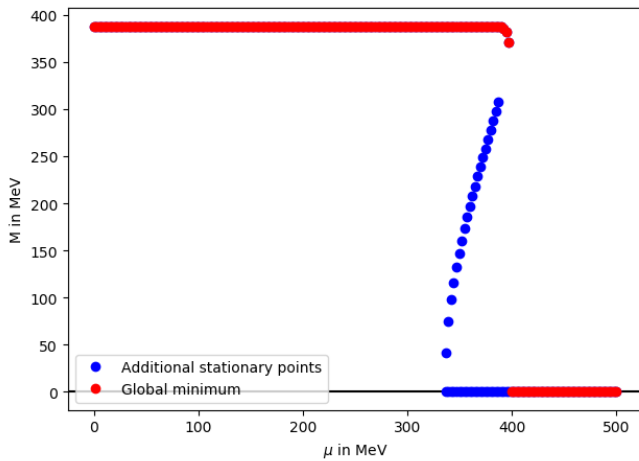


(a) Chiral limit

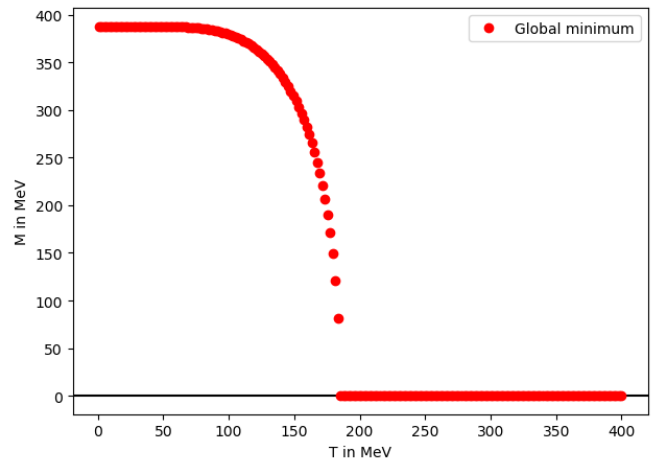


(b) Finite bare mass

Abbildung 4.4.: Thermodynamic potential of the NJL-model in dependence of the order parameter M in the case of the critical endpoint. It can be seen, that the potential is relatively flat over a long interval.



(a) First order phase transition

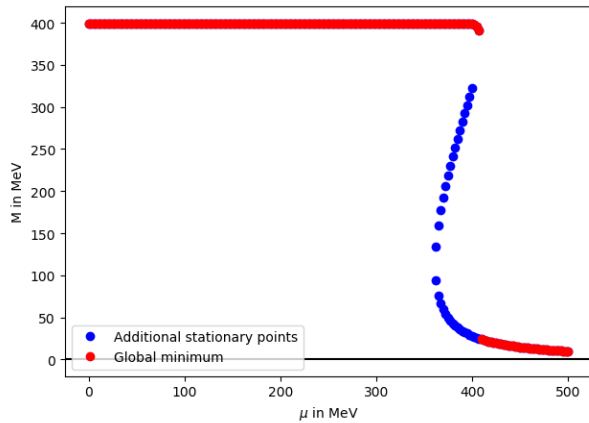


(b) Second order phase transition

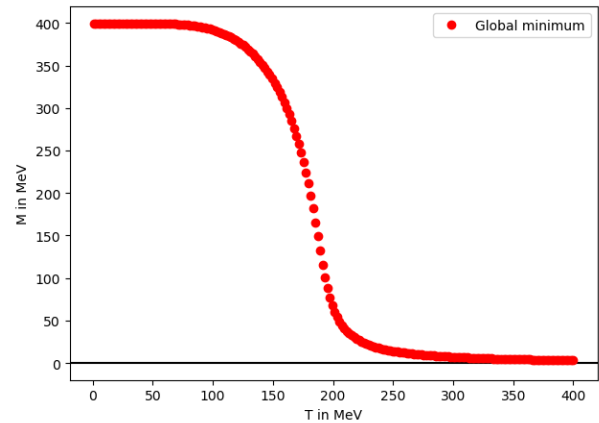
Abbildung 4.5.: The behavior of the order parameter M in case of a first and second order phase transition in the chiral limit. In both cases M goes exactly to zero after the phase transition. Shortly before the first order phase transition takes place, multiple values of M have stationary points in the thermodynamic potential with red representing the global minimum.

With the thermodynamic potential on hand it is now possible to calculate the effective quark mass for a given T and μ . This can be done by searching for the global minimum of the thermodynamic potential in regards to M . The behavior of the effective mass in the chiral limit in case of a first and second order phase transition can be seen in figure 4.5. Notably in both cases the effective mass goes exactly to zero after the phase transition. At some points with the first order phase transition the potential can have multiple stationary points of interest. All these points can be seen with the point of global minimum colored red. In case of the second order phase transition one can see that around the phase border the curve of the effective mass gets very steep, until it can look like a first order phase transition with the given resolution. This can make the determination of the position of the critical endpoint tricky, which is why the next chapter will discuss another method of determining its position.

Lastly figure 4.6 shows the effective mass in case of finite bare mass. In contrast to the case of chiral limit the mass does not go exactly to zero after the phase transition. Otherwise the situation is very similar to the case of chiral limit.



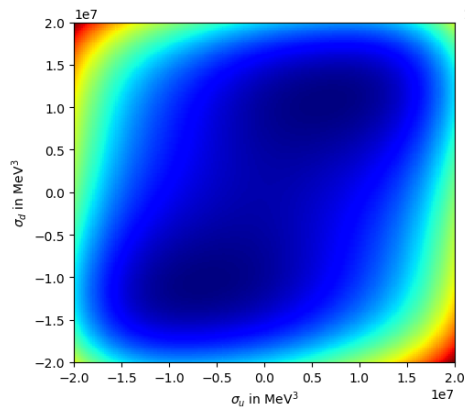
(a) First order phase transition



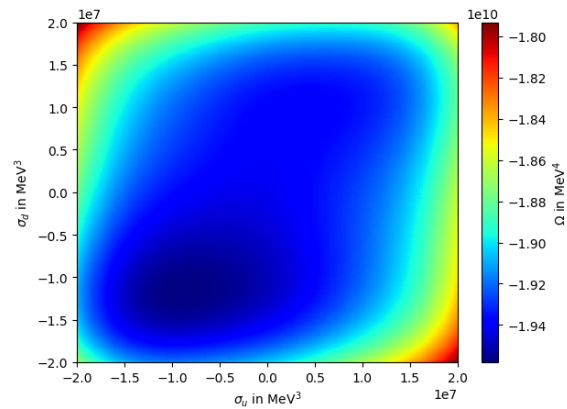
(b) Second order phase transition

Abbildung 4.6.: The behavior of the order parameter M in case of a first and second order phase transition with finite bare mass. In both cases M stays finite, even after the phase transition. Shortly before the first order phase transition takes place, multiple values of M have stationary points in the thermodynamic potential with red representing the global minimum.

Finite isospinchemical potential



(a) Chiral limit



(b) Finite bare mass

Abbildung 4.7.: The thermodynamic potential for finite isospinchemical potential with $\kappa = 0.05$, $T = 100$ MeV and $\mu = 270$ MeV.

Figure 4.7 showcases the form of the thermodynamic potential, in case the isospinchemical potential is finite. The x- and y-axis correspond to the values of the quark condensates. Again one can see the symmetry of the potential in case of the chiral limit. The forms are very similar to the form seen in figure 4.2 and 4.3, the difference being that the potential now deepens on more than one variable.

As before one can now calculate the effective masses for different μ and T . The first order phase transition under similar conditions as figures 4.5a and 4.6a can be seen in figure 4.8. The transition is seen at different values of κ . If the value of κ is low enough, two separate phase transitions can be seen. As κ gets bigger these transitions move closer together, until only one transition takes place. The other features of the transitions are just like the case of zero isospinchemical potential.

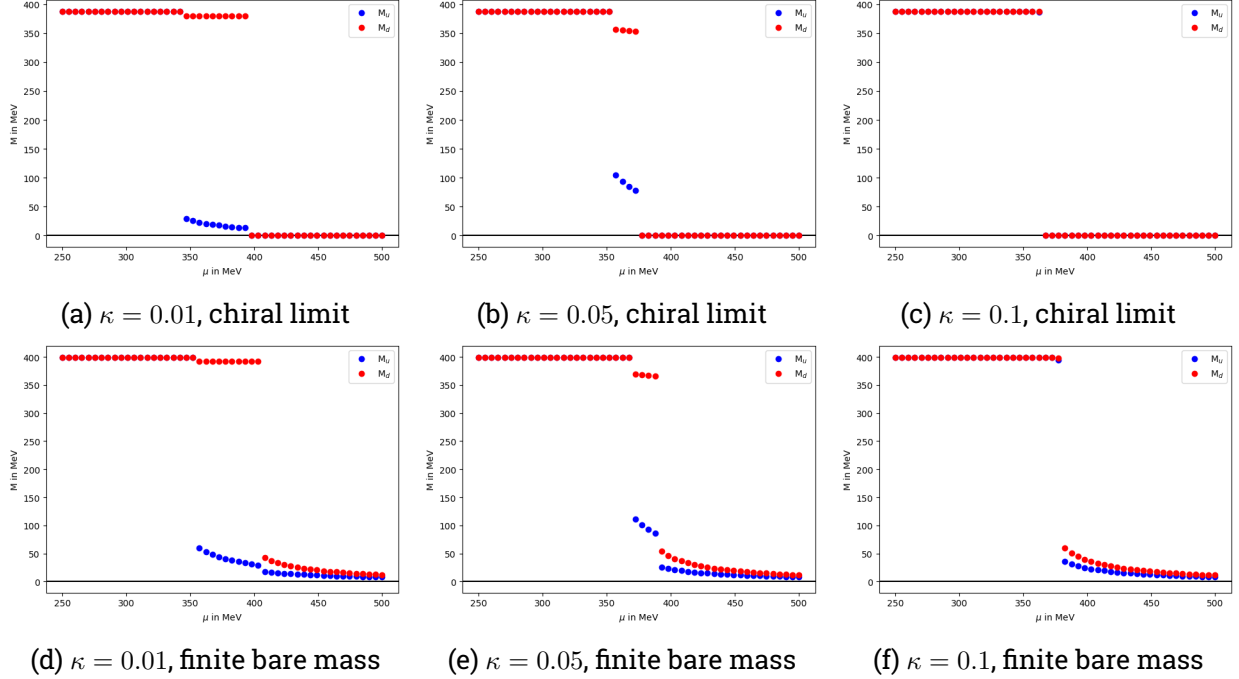


Abbildung 4.8.: The first order phase transition for different κ at $T = 0$. For small κ two transitions take place with the difference between them shrinking until only one transition happens.

If the second order phase transition for $\mu = 0$ is plotted, both M_u and M_d have the same values. For this reason $\mu = 200$ MeV was chosen, such that one can see a difference to the case of zero isospinchemical potential. One feature of the chiral limit can both be seen in the first and second order phase transitions. From the gap equation and the self consistent conditional equation of the quark condensates it can be derived, that one effective mass being zero results on the other one being zero as well. In case of first order phase transition this means, that even after the first transition one condensate cannot be zero, until the other one is also zero, after the second phase transition. In the case of second order phase transition, this means both effective masses reach zero at the same time.

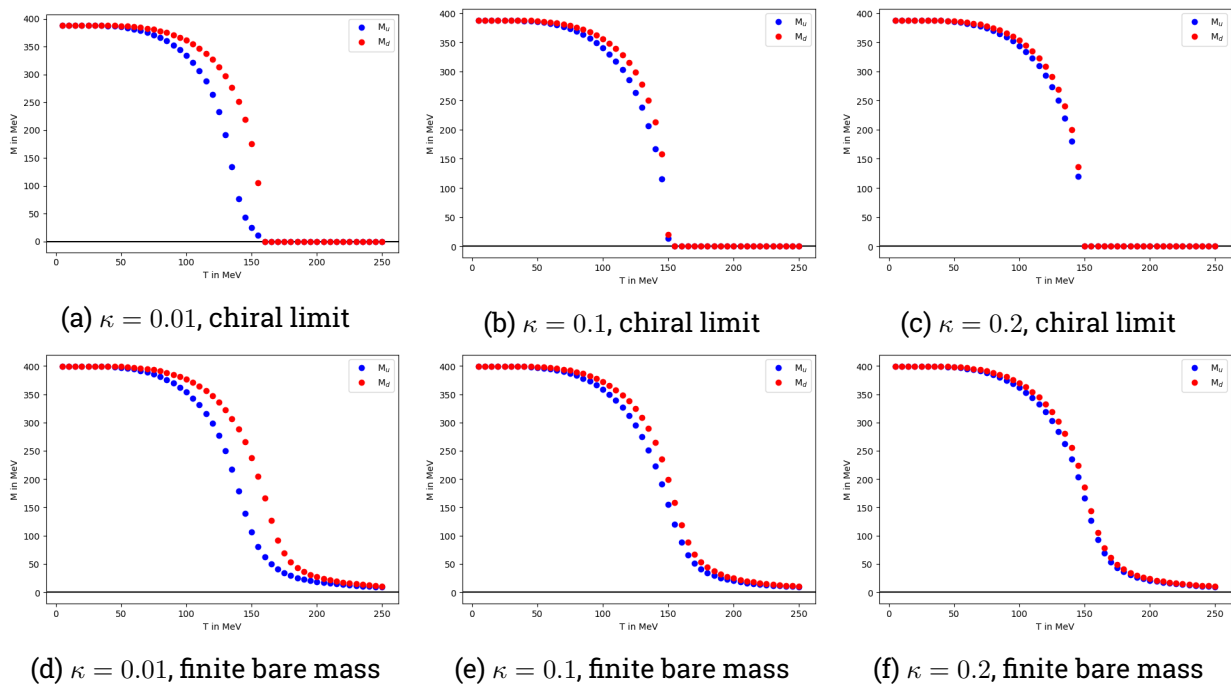


Abbildung 4.9.: The second order phase transition for different κ at $\mu = 200$ MeV. If the chemical potential is zero, both effective masses behave exactly the same way, which is why a finite chemical potential was chosen.

5. Ginzburg-Landau analysis

When phase transitions are discussed it can be hard to determine, if the transition is of first or second order. This impedes the search for the critical endpoint in the QCD phase diagram. The Ginzburg-Landau (GL) analysis can be used to find the position of the critical endpoint to any wanted precision. It can be derived from the GL theory, a mathematical physical continuum description of phase transitions, which was first developed by V. Ginzburg, L. Landau, A. Abrikosov and L. Gorkov to describe the phase transition in superconductors [9].

For this thesis, in which the order parameter does not depend on spatial position, the general idea of the GL analysis is to develop the thermodynamic potential in a Taylor series. In this regard four slightly different cases will be discussed later on.

5.1. General points

The chosen order parameters, the constituent quark masses M_u and M_d , are without spacial dependence. This means the thermodynamic potential can be expanded in the following way:

$$\Omega_{NJL}[M] = \sum_{n \in \mathbb{N}_0} \alpha_n(T, \mu) \cdot (M - M_0)^n \quad (5.1)$$

In this expression M_0 denotes the effective mass around which the potential is expanded. This point will correspond in the following to a stationary point of the potential, so it is a solution of the gap equation. The Ginzburg-Landau coefficients α_n depend on T and μ and can be obtained by the the partial derivative of the thermodynamic potential with respect to the constituent mass:

$$\alpha_n(T, \mu) = \frac{1}{n!} \frac{\partial^n \Omega_{NJL}(T, \mu; M)}{\partial M^n} \Big|_{M=M_0} \quad (5.2)$$

This means in the following discussions α_1 will always be equal to zero, because this is a requirement for a stationary point. These are the general ideas which will be used to calculate the critical endpoint with different conditions in the next sections.

5.2. Analysis in the chiral limit with no isospinchemical potential

This case is the simplest of the in this thesis discussed cases. The reason for this is, because the field of the up- and down-quark behave the same way and furthermore the trivial solution $M_0 = 0$ can be chosen as an evaluation point. Additionally the chiral symmetry is intact. That means the thermodynamic potential is an even function in regard to M . It follows, that all odd coefficients are zero and the expansion can be simplified to

$$\Omega_{NJL}[M] = \sum_{n \in \mathbb{N}_0} \alpha_{2n}(T, \mu) \cdot M^{2n}. \quad (5.3)$$

Furthermore it can be assumed, that the coefficients of order six or higher are positive. This leaves α_2 and α_4 to be investigated further.

5.2.1. The Ginzburg-Landau coefficients

Using equation 5.2 the coefficients can be calculated. This gives for α_2 :

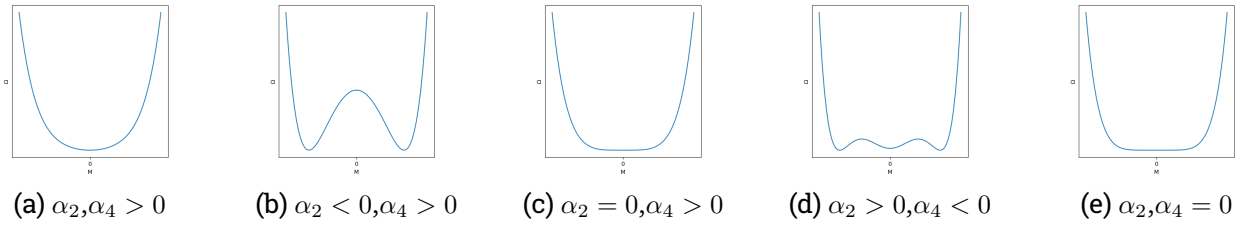
$$\alpha_2(T, \mu) = \frac{1}{4G} - \frac{3}{\pi^2} \cdot \left(\frac{\Lambda^2}{2} - \int_0^\infty dp p (n_{\bar{p},f} + \bar{n}_{\bar{p},f}) \right) \quad (5.4)$$

α_4 can be calculated to be

$$\alpha_4(T, \mu) = -\frac{1}{4\pi} \left[3 - \int_0^\Lambda dp \frac{3}{p} + \int_0^\infty dp \frac{3}{p} (n_{\bar{p},f} + \bar{n}_{\bar{p},f}) \right] \quad (5.5)$$

In this expression the first integral is infrared divergent, but when combined with the second integral this divergence does not occur.

The next step to compute the critical endpoint is to understand the behavior of the thermodynamic potential in relation to these coefficients.



Abbildungung 5.1.: The qualitative behavior of the thermodynamic potential in the chiral limit under varying sign of the important GL coefficients.

For this one has to consider the sign of all of the coefficients. As mentioned before the sign of the coefficients greater or equal to order six is positive. The sign of α_2 and α_4 can vary. This leaves five important cases to discuss. The different forms of the potential in these cases can be seen in figure 5.1. If α_2 as well as α_4 are greater than zero, then the potential has only one stationary point at $M = 0$. This means the potential is in the restored phase, which is seen in figure 5.1a. When α_4 is positive, but α_2 is negative, the potential takes the form of a W. This means some $M > 0$ is preferred over the trivial solution as seen in the second picture. The closer α_2 is to zero, the smaller the difference between the maximum and the minima gets and the closer the position of the minima gets to $M = 0$, until a phase transition of second order happens at $\alpha_2 = 0$. The next case to consider is $\alpha_2 > 0$ and $\alpha_4 < 0$. This leads to five stationary points in total, three of which are minima, as seen in figure 5.1d. With this setup only a first order phase transition can happen. In conclusion this means the critical endpoint is at the point at which the first and second order phase transition meet, which leads to the condition:

$$\alpha_2(T, \mu) = \alpha_4(T, \mu) \stackrel{!}{=} 0 \quad (5.6)$$

With this one can determine the position of the critical endpoint to any wanted precision.

5.2.2. Diagram of Ginzburg-Landau coefficients

In figure 5.2 the curves on which α_2 and α_4 are zero can be seen. The point at which these curves meet is the critical endpoint. The curve of $\alpha_2 = 0$ corresponds to the border of second order phase transition in the part of the diagram, which is left to the critical endpoint. The coordinates of the critical endpoint are $T = 112.78$ MeV and $\mu = 266.04$ MeV.

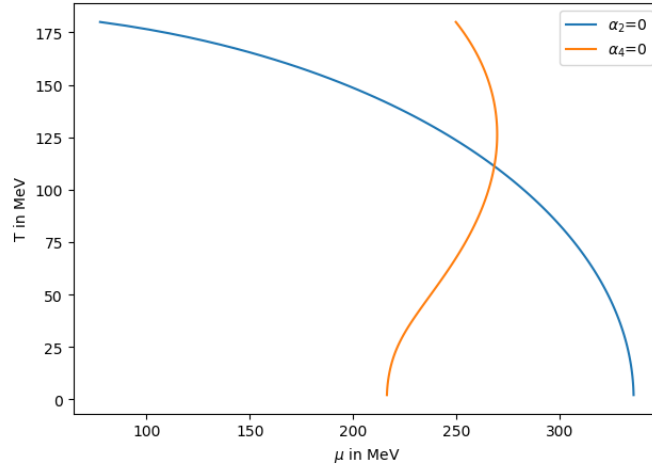


Abbildung 5.2.: Phase diagram with GL coefficients in the chiral limit with zero isospinchemical potential. The critical endpoint is located at the intersection of the lines.

5.3. Analysis in the chiral limit and finite isospinchemical potential

In this section the arguments of the last section still hold true, but the thermodynamic potential which has to be considered is more complex. It now depends on two variables, which leads to a two dimensional Taylor series

$$\Omega_{NJL}[\sigma_u, \sigma_d] = \sum_{n \in \mathbb{N}_0} \sum_{m \in \mathbb{N}_0} \alpha_{n,m}(T, \mu) \cdot \sigma_u^n \cdot \sigma_d^m \quad (5.7)$$

with the coefficients given by

$$\alpha_{n,m}(T, \mu) = \frac{\binom{n+m}{n}}{(n+m)!} \left. \frac{\partial^{n+m} \Omega_{NJL}(T, \mu; \sigma_u, \sigma_d)}{\partial \sigma_u^n \partial \sigma_d^m} \right|_{\sigma_u=0, \sigma_d=0} \quad (5.8)$$

As mentioned $\sigma_u = \sigma_d = 0$ can still be used as an evaluation points and only coefficients of even order are different from zero. The order in this case is determined by the sum of m and n . In addition the order parameter is now given by the quark condensates and not the effective masses of the quarks. This is only a technicality, which makes calculations easier, and the gap equations 4.17 and 4.18 give a linear conversion between the two representations.

5.3.1. Calculating the Ginzburg-Landau coefficients

To calculate the GL-coefficients it is more practical to rewrite the derivatives of Ω_{NJL} in regard to σ_u and σ_d to derivatives in regard to the effective masses in the following way:

$$\alpha_{n,m} = \frac{\binom{n+m}{n}}{(n+m)!} \left(C + \frac{\partial^{n+m} \Omega_0(T, \mu; M_u)}{\partial \sigma_u^n \partial \sigma_d^m} \Big|_{\sigma_u=\sigma_u,0, \sigma_d=\sigma_d,0} + \frac{\partial^{n+m} \Omega_0(T, \mu; M_d)}{\partial \sigma_u^n \partial \sigma_d^m} \Big|_{\sigma_u=\sigma_u,0, \sigma_d=\sigma_d,0} \right) \quad (5.9)$$

$$= b \cdot \left[C + \left(\frac{\partial M_u}{\partial \sigma_u} \right)^n \left(\frac{\partial M_u}{\partial \sigma_d} \right)^m \frac{\partial^{n+m} \Omega_0}{\partial M_u^{n+m}} \Big|_{M_u=M_u,0} + \left(\frac{\partial M_d}{\partial \sigma_u} \right)^n \left(\frac{\partial M_d}{\partial \sigma_d} \right)^m \frac{\partial^{n+m} \Omega_0}{\partial M_d^{n+m}} \Big|_{M_d=M_d,0} \right] \\ = b \cdot \left[C + (-4G_1)^n (-4G_2)^m \frac{\partial^{n+m} \Omega_0}{\partial M_u^{n+m}} \Big|_{M_u=M_u,0} + (-4G_2)^n (-4G_1)^m \frac{\partial^{n+m} \Omega_0}{\partial M_d^{n+m}} \Big|_{M_d=M_d,0} \right] \quad (5.10)$$

The constant C depends on m and n :

$$C = \begin{cases} 4G_1, & \text{if } n = 2, m = 0 \text{ or } n = 0, m = 2 \\ 4G_2, & \text{if } n = 1, m = 1 \\ 0, & \text{else} \end{cases}$$

For overview purposes the coefficients will not be written out, but the important derivatives of the thermodynamic potential can be found in the appendix, with which the coefficients can be calculated.

5.3.2. Conditions for the critical endpoint

The goal of this part is to find a condition for the critical endpoint, similar to equation 5.6. Now the thermodynamic potential depends on two instead of one variable. To analyze this one has to consider multidimensional analysis. The equivalent to the second derivative is given by the Hesse-matrix. In this case the Hesse-matrix takes the following form:

$$H_{\Omega_{NJL}} = \begin{pmatrix} \alpha_{2,0} & \frac{\alpha_{1,1}}{2} \\ \frac{\alpha_{1,1}}{2} & \alpha_{0,2} \end{pmatrix} \quad (5.11)$$

If a multidimensional function has a minimum the Hesse-matrix at this point has to be positive-definite. This is the case, if all eigenvalues are greater than zero. On the other hand if the Hesse-matrix is not definite, which means some eigenvalues are greater and some are less than zero, the function has a saddle point. The eigenvalues of the matrix given by 5.11 can be calculated by

$$\lambda_{\pm} = \frac{1}{2} \left((\alpha_{2,0} + \alpha_{0,2}) \pm \sqrt{(\alpha_{2,0} - \alpha_{0,2})^2 + \alpha_{1,1}^2} \right) \quad (5.12)$$

This leads to three cases. If $\alpha_{2,0} + \alpha_{0,2} < 0$, then λ_- will always be less than zero. This means the stationary point will never be a minimum. In the other cases $\alpha_{2,0} + \alpha_{0,2}$ has to be greater than zero. This means λ_+ is always positive. The second case is then given by λ_- being less than zero, which again means the stationary point is not a minimum, but if λ_- is greater than zero the conditions for a minimum are met. The last case is equivalent to the following condition:

$$4 \cdot \alpha_{2,0} \cdot \alpha_{0,2} > \alpha_{1,1}^2 \quad (5.13)$$

In conclusion this leads to the following set of conditions for the second order phase transition:

$$4 \cdot \alpha_{2,0} \cdot \alpha_{0,2} - \alpha_{1,1}^2 = 0 \text{ and } \alpha_{2,0}, \alpha_{0,2} \geq 0 \quad (5.14)$$

This means the critical endpoint has to live on the curve which is given by one eigenvalue of the Hesse-matrix being equal to zero. From this a relation between σ_u and σ_d can be derived:

$$\begin{pmatrix} \alpha_{2,0} & \frac{\alpha_{1,1}}{2} \\ \frac{\alpha_{1,1}}{2} & \alpha_{0,2} \end{pmatrix} \begin{pmatrix} \sigma_u \\ \sigma_d \end{pmatrix} = 0 \quad (5.15)$$

$$\Rightarrow \sigma_d = -\frac{2\alpha_{2,0}}{\alpha_{1,1}}\sigma_u = -\frac{\alpha_{1,1}}{2\alpha_{0,2}}\sigma_u \quad (5.16)$$

The factors in 5.16 are the same, because the conditions in 5.14 still hold true. With this relation the terms of second order in 5.7 can be summarized in the following way:

$$\alpha_{2,0} \cdot \sigma_u^2 + \alpha_{1,1} \cdot \sigma_u \cdot \sigma_d + \alpha_{0,2} \cdot \sigma_d^2 \quad (5.17)$$

$$= \left[\alpha_{2,0} - \alpha_{1,1} \cdot \frac{2\alpha_{2,0}}{\alpha_{1,1}} + \alpha_{0,2} \cdot \left(\frac{2\alpha_{2,0}}{\alpha_{1,1}} \right)^2 \right] \cdot \sigma_u \quad (5.18)$$

$$= \alpha_{2,0} \left(\frac{4 \cdot \alpha_{2,0} \cdot \alpha_{0,2}}{\alpha_{1,1}^2} - 1 \right) \cdot \sigma_d^2 \quad (5.19)$$

$$=: \tilde{\alpha}_2 \cdot \sigma_d^2 \quad (5.20)$$

The same can be done with the terms of fourth order, which leads to the following definition:

$$\tilde{\alpha}_4 := \alpha_{4,0} - \alpha_{3,1} \cdot \frac{2\alpha_{2,0}}{\alpha_{1,1}} + \alpha_{2,2} \cdot \left(\frac{2\alpha_{2,0}}{\alpha_{1,1}} \right)^2 - \alpha_{1,3} \cdot \left(\frac{2\alpha_{2,0}}{\alpha_{1,1}} \right)^3 + \alpha_{0,4} \cdot \left(\frac{2\alpha_{2,0}}{\alpha_{1,1}} \right)^4 \quad (5.21)$$

With these definitions the condition for the critical endpoint can be written analogous to 5.6:

$$\tilde{\alpha}_2(T, \mu) = \tilde{\alpha}_4(T, \mu) \stackrel{!}{=} 0 \quad (5.22)$$

With equation 5.19 it is easy to see, that $\tilde{\alpha}_2$ being equal to zero is the same as condition 5.14. It is important to note, that the current definitions only allow to determine the critical endpoint of the phase transition of the later condensate. This can be circumvented by not fixating the expansion point. This method will be discussed later in the case of non zero bare mass, where it becomes mandatory.

5.3.3. Diagram of Ginzburg-Landau coefficients

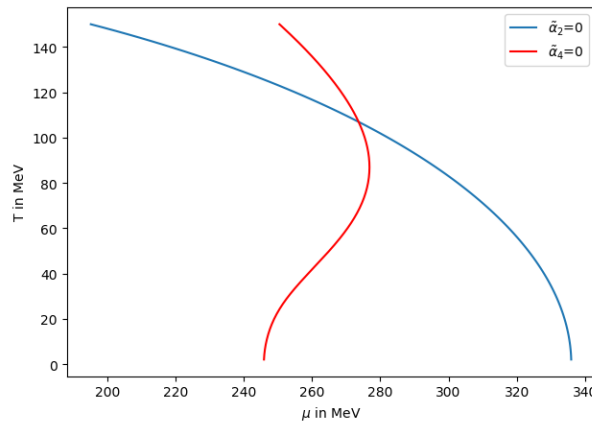
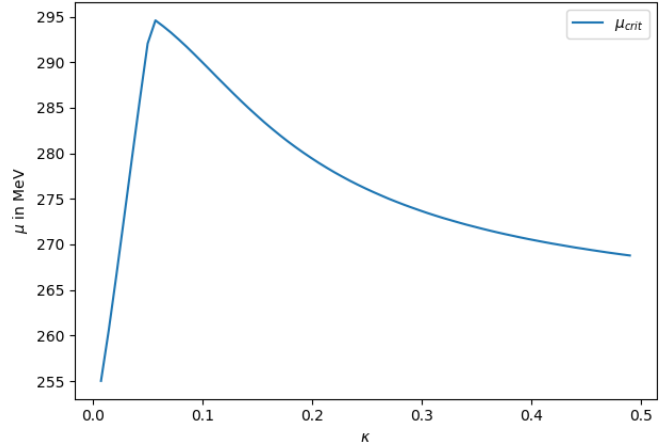
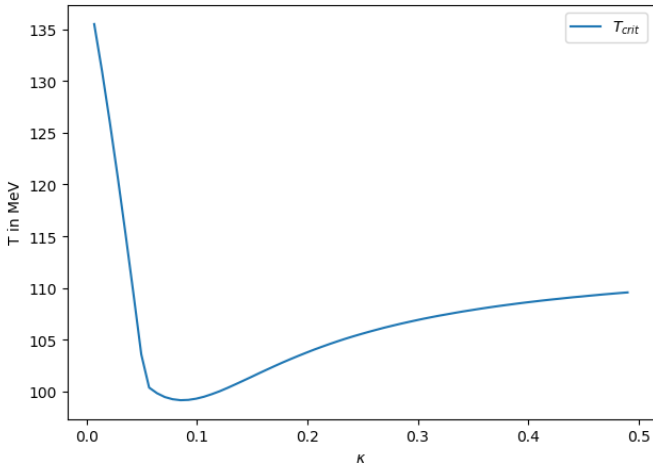


Abbildung 5.3.: Phase diagram with GL coefficients in the chiral limit with finite isospinchemical potential and $\kappa = 0.3$. The critical endpoint is located at the intersection of the lines.

An example of the curves with $\tilde{\alpha}_2$ and $\tilde{\alpha}_4$ being equal to zero can be seen in figure 5.3. For this $\kappa = 0.3$ was chosen. It can be seen, that the form of the curves is very similar to the case of zero isospinchemical potential. The critical point in this diagram is at position $T = 106.92$ MeV and $\mu = 273.65$ MeV.



(a) Temperature of the critical point in dependence of κ

(b) Chemical potential of the critical point in dependence of κ

Abbildung 5.4.: Temperature and chemical potential of the critical point in dependence of κ in the chiral limit.

With this method one can now determine the position of the critical point for different values of κ . The resulting diagrams can be seen in figure 5.4. One can see, that the temperature of the critical point first goes down, as the value of κ increases, then has a minimum for $\kappa \approx 0.08$ after which the temperature rises steadily until the end. The chemical potential of the critical point shows the opposite behavior, first rising and then falling. This reversed behavior of the temperature and chemical potential is to be expected, because as the temperature gets lower the phase transition moves to higher chemical potentials. As κ approaches the limit case of $\kappa = \frac{1}{2}$ the temperature as well as the chemical potential reach the same values as the critical point in the case of zero isospinchemical potential, which is as expected. Interestingly the temperature for the other limit case, $\kappa = 0$ does not approach the same temperature as in the case of zero isospinchemical potential. This may be a sign of some problems with the numeric calculations in this case, because as one can see in the next sections, in the case of finite bare mass this limit case behaves as expected.

5.4. Finite bare mass with no isospinchemical potential

With the mass of the quarks being finite and not zero the phase is no longer exactly restored, which complicates the situation. This means $M_0 = 0$ can no longer be used as the expansion point like in section 5.2. Instead one must calculate a stationary point around which the thermodynamic potential can be expanded. This has to be done by solving the gap equation for a given T and μ , which means the expansion takes the following form:

$$\Omega_{NJL}[M] = \sum_{n \in \mathbb{N}_0} \alpha_n(T, \mu) \cdot (M - M_0(T, \mu))^n \quad (5.23)$$

With the coefficients still given by equation 5.2. As mentioned before α_1 is equal to zero, since $M_0(T, \mu)$ is still a stationary point of the potential. All other coefficients are in general not equal to zero and have to be considered, because the symmetry argument does not apply anymore. Similar ideas as in section 5.2.1 can be used to get a new condition for the critical endpoint using α_2 and α_3 .

5.4.1. The Ginzburg-Landau coefficients

With the expansion point $M_0(T, \mu)$ not being equal to zero the formulas for the coefficients get much more complex, which is why they will not be shown here, but the important derivatives of the thermodynamic potential can be found in the appendix from which the coefficients can be easily derived.

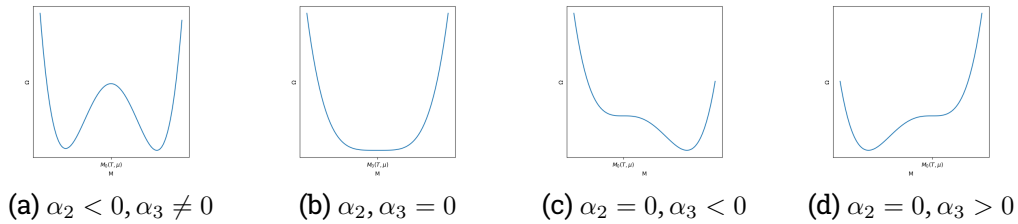


Abbildung 5.5.: The qualitative behavior of the thermodynamic potential with finite bare mass under varying sign of the important GL coefficients.

Just like in chiral limit the behavior of the potential depending on the sign of α_2 and α_3 and can be seen in figure 5.5. It is again assumed, that all coefficients of order four or higher are greater than zero. The first picture represents the form of the potential at a point of first order phase transition. The potential has three stationary points, two of which are minima and one maximum. If one moves along this curve the three stationary point will move closer together until they merge at the point at which $\alpha_2 = 0$. This point can be seen in the second picture and is the searched critical endpoint. Conversely if α_2 is equal to zero the one gets the left spinodale, if $\alpha_3 < 0$, as seen in the third picture, figure 5.5c, or the right spinodale, if $\alpha_3 > 0$ as seen in the last picture, figure 5.5d. The left and right spinodale meet at the critical endpoint, which makes it necessary for α_3 to be equal to zero at this point. This means the condition for the critical endpoint is again similar to the cases before and given by:

$$\alpha_2(T, \mu) = \alpha_3(T, \mu) \stackrel{!}{=} 0 \quad (5.24)$$

With this condition one can again look for the critical endpoint to any wanted precision.

5.4.2. Diagram of Ginzburg-Landau coefficients

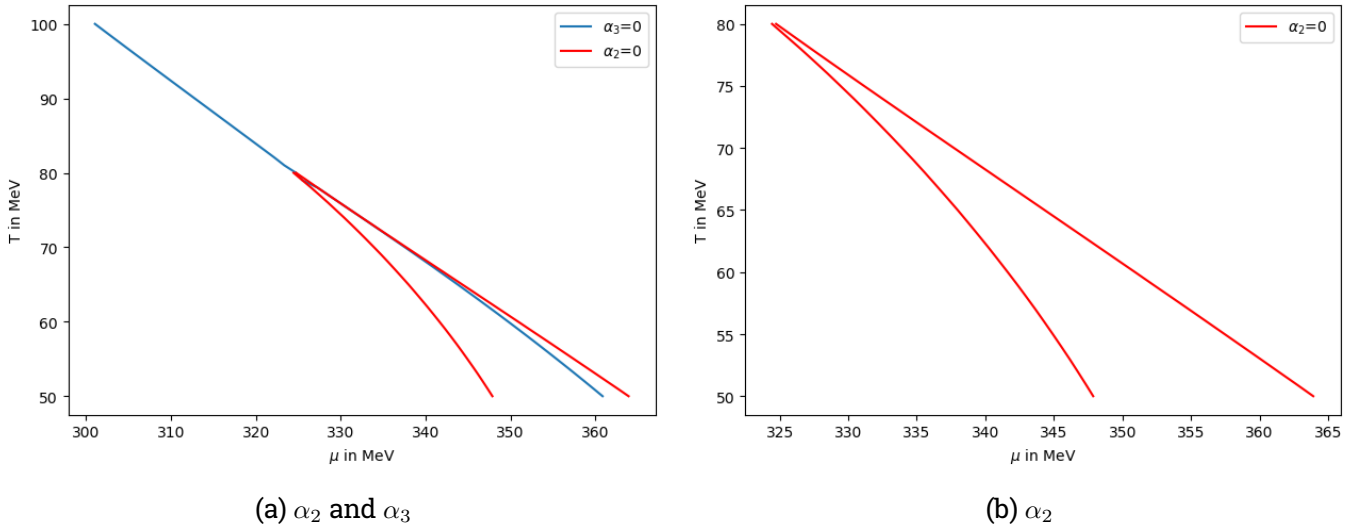


Abbildung 5.6.: Phase diagram with GL coefficients with finite bare mass and zero isospinchemical potential. As seen by comparing the first and second picture, the critical endpoint is easier to calculate by searching the temperature at which α_2 has no root.

The resulting diagrams of the Ginzburg-Landau coefficients can be seen in figure 5.6. The first picture shows both coefficients. This time α_2 can have two or zero points per temperature at which it is zero. The two points are the left and right spinodale of the phase transition. One can see, that the two curves are very close to each other, which makes it harder to find the exact point at which they meet. For this reason α_3 can be disregarded and one can look for the temperature at which α_2 has no root to find the critical endpoint. With this method the coordinates of the endpoint can be calculated to be $T = 81.63$ MeV and $\mu = 322.65$ MeV.

5.5. Finite bare mass and finite isospinchemical potential

This section will combine the modifications, which were made by the last two sections. This means the point of expansion for a given T and μ has to be calculated and $\tilde{\alpha}_2$ will be used as defined by equation 5.19 instead of α_2 . The GL coefficients behave very similar to the case of zero isospinchemical potential. For this reason $\tilde{\alpha}_3$ will not be considered, because the critical point can be calculated better with $\tilde{\alpha}_2$ alone. In contrast to the case of finite isospinchemical potential and chiral limit one can now compute the critical endpoints of both condensates, because not only the trivial solution is considered as an expansion point of the thermodynamic potential. In this section the regularization parameters given by equations 4.38 to 4.40 are used, to compare the results to past calculations. One example of the phase diagram with $\tilde{\alpha}_2 = 0$ in the case of $\kappa = 0.05$ can be seen in figure 5.7. It is similar to the case of zero isospinchemical potential, but a second phase transition can be seen, which means for some κ two critical endpoints can be calculated.

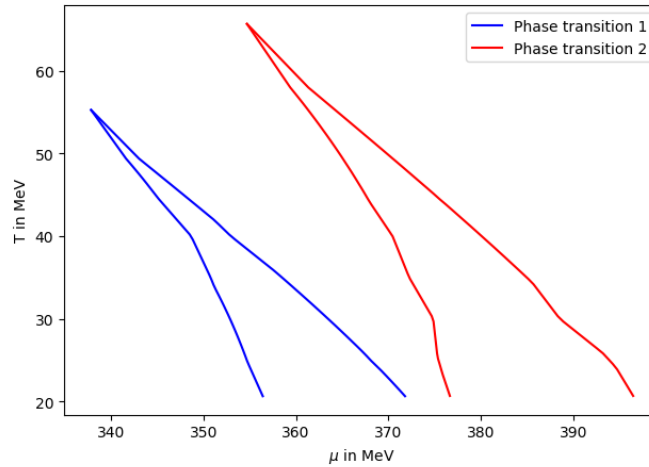
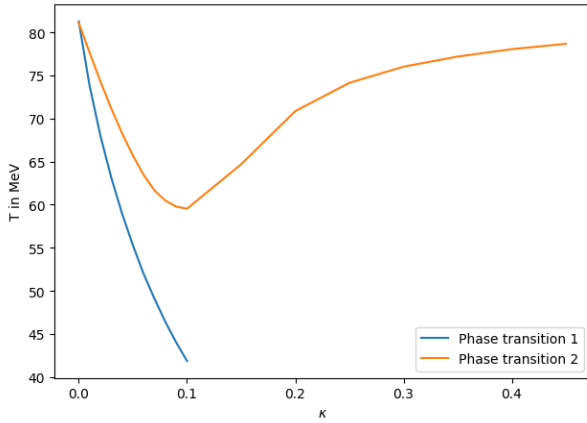
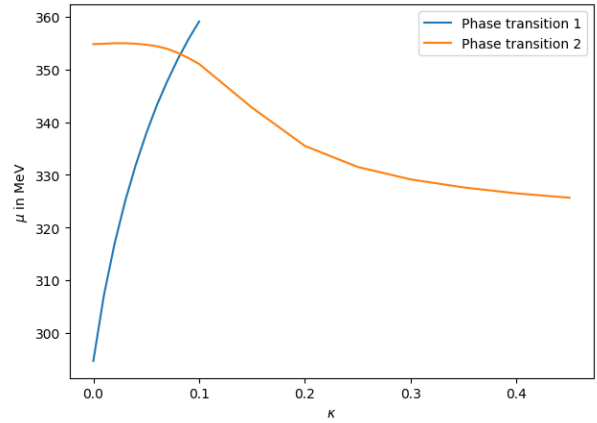


Abbildung 5.7.: Phase diagram with GL coefficients with finite bare mass and finite isospinchemical potential with $\kappa = 0.05$. The coefficient $\tilde{\alpha}_2$ can have up to four roots, with two critical endpoints.

With this in mind one can now calculate the positions of the critical endpoints for one given κ . The behavior of these points can be seen in figure 5.8. One can see, that in comparison to the chiral limit case both $\kappa = 0$ and $\kappa = \frac{1}{2}$ result in the same temperature of the phase transition. When one does calculations with the same regularization parameters as in section 5.4.2 for $\kappa = 0$, the temperature of the critical point can be calculated to be $T = 82.2$ MeV. This is approximately the same as in the case of zero isospinchemical potential. The form of the temperature curve of the second phase transition behaves similar to the curve in the chiral limit, the difference being for low values of κ . With the dynamic evaluation point the critical point of the other phase transition can be calculated. The temperature of this critical point gets lower and lower until it completely vanishes. This vanishing happens at $\kappa \approx 0,1175$. Interestingly the temperature of the first phase transition gets low enough, that the value of μ at this critical point is higher than the value of μ for the critical point of the second phase transition.



(a) Temperature of the critical point in dependence of κ



(b) Chemical potential of the critical point in dependence of κ

Abbildung 5.8.: Temperature and chemical potential of the critical points in dependence of κ for finite bare mass.

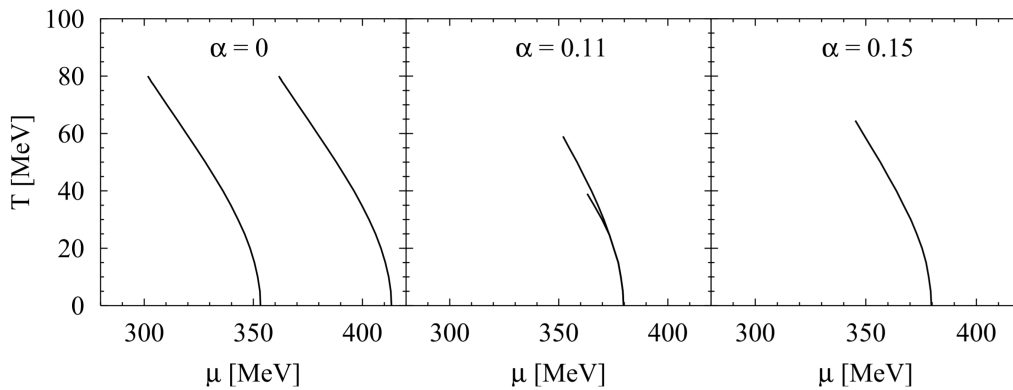


Abbildung 5.9.: Phase diagram with first order phase transition border with finite bare mass and isospinchemical potential. The coefficient α corresponds to the coefficient κ of this thesis. These diagrams were taken from [10] to compare them to current calculations.

Lastly these calculations can now be compared to past calculations. Figure 5.9 shows phase diagrams of the QCD with the border of first order phase transition drawn. The critical endpoint is the endpoint of this curve. The parameter α corresponds to the parameter κ of this thesis. From these diagrams one can get the approximate position of the critical endpoints. In the case $\kappa = 0$ one can get the following positions of the critical endpoints from the diagram

$$T_{C,1} \approx 80 \text{ MeV and } \mu_{C,1} \approx 305 \text{ MeV} \quad (5.25)$$

$$T_{C,2} \approx 80 \text{ MeV and } \mu_{C,2} \approx 365 \text{ MeV} \quad (5.26)$$

By comparison the in this thesis calculated positions are

$$T_{C,1} = 81.3 \text{ MeV and } \mu_{C,1} = 294.6 \text{ MeV} \quad (5.27)$$

$$T_{C,2} = 81.1 \text{ MeV and } \mu_{C,2} = 354.8 \text{ MeV} \quad (5.28)$$

The temperatures are nearly the same, but interestingly the chemical potentials differ by around 10 MeV. For $\kappa = 0.15$ the diagram shows

$$T_{C,3} \approx 64 \text{ MeV and } \mu_{C,3} \approx 345 \text{ MeV} \quad (5.29)$$

With the calculations giving

$$T_{C,3} = 64.9 \text{ MeV and } \mu_{C,3} = 342.7 \text{ MeV} \quad (5.30)$$

Which is nearly the same. With this one can conclude that both methods give the same results, but the exact positions of the critical endpoint can be determined more easily and efficient by the Ginzburg-Landau analysis.

6. Conclusion and outlook

The goal of this thesis was to calculate the critical endpoints of the QCD phase diagram for finite isospin-chemical potential via the Ginzburg-Landau analysis. So far these calculations were only done with zero isospin-chemical potential. For this the NJL-model, a low energy effective theory of QCD, was introduced in chapter 4 and the symmetries of a simpler form of its Lagrangian were discussed. After that a more generalized Lagrangian seen in equation 4.5, which allows finite isospin-chemical potential, was introduced and with the mean field approximation equation 4.26 for the thermodynamic potential of the NJL-model was derived.

In the next step section 4.4.2 discussed the properties of this thermodynamic potential for zero isospin-chemical potential to understand the behavior of the order parameter, the effective quark mass, in case of a first and second order phase transition. After that these behaviors were examined closer in different cases. These cases were the chiral limit, which means with the bare mass of the quarks being equal to zero, with finite bare mass, with zero isospin-chemical potential and with finite isospin-chemical potentials. All possible combinations of these were considered to understand the behavior of the order parameter for first and second order phase transitions.

In the last chapter the thermodynamic potential was examined with the Ginzburg-Landau analysis, to find the position of the critical endpoint in the QCD phase diagram. For this first the case of zero isospin-chemical potential and bare mass was discussed and condition 5.6 for the Ginzburg-Landau coefficients was derived, with which the position of the critical endpoint was calculated to be $T = 112.78$ MeV and $\mu = 266.04$ MeV. The Ginzburg-Landau analysis was next generalized to allow finite isospin-chemical potentials. With this new coefficients were derived, with which a new condition, condition 5.22, for the critical endpoint in the same form as the condition for zero isospin-chemical potential was derived. With this condition the critical endpoint was calculated for different values of κ . The behavior of the temperature and the chemical potential of the critical are displayed in figure 5.4. In the next step the case of finite bare mass and zero isospin-chemical potential was considered. A new condition 5.24 with different Ginzburg-Landau coefficients was found. After computing the phase diagram with the new coefficients in figure 5.6 it got apparent, that only one of these coefficients was relevant to calculate the critical endpoint. With this the position of the critical endpoint was computed to be $T = 81.63$ MeV and $\mu = 322.65$ MeV.

With the generalizations for finite isospin-chemical potential and finite bare mass combined the final case was examined. The expansion point was calculated newly for every T and μ , which made it possible to calculate the critical endpoint for both occurring phase transitions. Like in the case of chiral limit the position of the endpoint depending on the value of κ could be calculated depicted in figure 5.8. These diagrams showed, that the first phase transition happens at lower and lower temperature with increasing value of κ until it vanishes. This happens at $\kappa \approx 0,1175$. Lastly the values of past calculations were compared to the results of this thesis, which showed that the values are approximately the same. This leads to the conclusion, that the Ginzburg-Landau analysis is a good method to calculate the critical endpoints in the QCD phase diagram.

In the course of this thesis many approximations were made, to simplify the calculations. To improve on these calculations one can for example consider the pion condensates, which were set to zero in the course of this thesis. Another obvious point of improvement is to let the order parameter vary for different spacial positions. Lastly the Lagrangian of the NJL-model can be further improved to allow more quark flavors and get a more general idea of the QCD phase diagram. But all in all the Ginzburg-Landau analysis seems to be a good way to understand more of the phase transition between the hadron phase and the QGP.

A. Derivatives of the thermodynamic potential

These are the general forms of the derivatives of the thermodynamic potential Ω_0 in regard to the effective quark mass.

The potential itself

$$\Omega_0(M, T, \mu) = -\frac{3}{\pi^2} \left(\int_0^\Lambda dp E_p + \int_0^\infty \left[T \ln(1 + \exp(-\frac{1}{T}(E_p - \mu))) + T \ln(1 + \exp(-\frac{1}{T}(E_p + \mu))) \right] \right) \quad (\text{A.1})$$

The first derivative

$$\frac{\partial \Omega_0(T, \mu; M)}{\partial M} = -\frac{3}{\pi^2} \cdot \left[\int_0^\Lambda dp \frac{p^2 M}{E_p} - \int_0^\infty dp \frac{p^2 M}{E_p} (n_{p,f} + \bar{n}_{p,f}) \right] \quad (\text{A.2})$$

The second derivative

$$\begin{aligned} \frac{\partial^2 \Omega_0(T, \mu; M)}{\partial M^2} = & -\frac{3}{\pi^2} \left(\int_0^\Lambda dp \frac{p^4}{E_p^3} \right. \\ & \left. - \int_0^\infty dp \left[\frac{p^4}{E_p^3} \cdot (n_{p,f} + \bar{n}_{p,f}) + \frac{p^2 M^2}{4 \cdot E_p^2 T} \cdot \left(\frac{1}{\cosh^2(\frac{E_p + \mu}{2T})} - \frac{1}{\cosh^2(\frac{E_p - \mu}{2T})} \right) \right] \right) \end{aligned} \quad (\text{A.3})$$

The second derivative at the point $M = 0$

$$\frac{\partial^2 \Omega_0(T, \mu; M)}{\partial M^2} \Big|_{M=0} = -\frac{3}{\pi^2} \left(\int_0^\Lambda dp p - \int_0^\infty dp p \cdot (n_{p,f} + \bar{n}_{p,f}) \right) \quad (\text{A.4})$$

The third derivative

$$\begin{aligned} \frac{\partial^3 \Omega_0(T, \mu; M)}{\partial M^3} = & -\frac{3}{\pi^2} \left[\int_0^\Lambda dp \frac{-3p^4 M}{E_p^5} \right. \\ & + \int_0^\infty dp \frac{p^4 M}{E_p^5} \cdot \left(\frac{E_p}{4T} \cdot \left(\frac{1}{\cosh^2(\frac{E_p - \mu}{2T})} + \frac{1}{\cosh^2(\frac{E_p + \mu}{2T})} \right) + 3 \cdot (n_{p,f} + \bar{n}_{p,f}) \right) \\ & + \frac{p^2}{2T} \cdot \left(\frac{M}{E_p^2} - \frac{M^3}{E_p^4} \right) \cdot \left(\frac{1}{\cosh^2(\frac{E_p + \mu}{2T})} + \frac{1}{\cosh^2(\frac{E_p - \mu}{2T})} \right) \\ & \left. - \frac{p^2 \cdot M^3}{4 \cdot E_p^3 T^2} \cdot \left(\frac{\tanh(\frac{E_p + \mu}{2T})}{\cosh^2(\frac{E_p + \mu}{2T})} + \frac{\tanh(\frac{E_p - \mu}{2T})}{\cosh^2(\frac{E_p - \mu}{2T})} \right) \right] \end{aligned} \quad (\text{A.5})$$

The forth derivative

$$\begin{aligned}
\frac{\partial^4 \Omega_0(T, \mu; M)}{\partial M^4} = & -\frac{3}{\pi^2} \left[\int_0^\Lambda dp - \frac{3p^4 \cdot (E_p^2 - 5M^2)}{E_p^7} \right. \\
& + \int_0^\infty dp \frac{p^4 \cdot (E_p^2 - 4M^2)}{4TE_p^6} \cdot \left(\frac{1}{\cosh^2(\frac{E_p+\mu}{2T})} + \frac{1}{\cosh^2(\frac{E_p-\mu}{2T})} \right) \\
& - \frac{p^4 M^2}{4T^2 E_p^5} \cdot \left(\frac{\tanh(\frac{E_p+\mu}{2T})}{\cosh^2(\frac{E_p+\mu}{2T})} + \frac{\tanh(\frac{E_p-\mu}{2T})}{\cosh^2(\frac{E_p-\mu}{2T})} \right) \\
& + \frac{3p^4 \cdot (E_p^2 - 5M^2)}{E_p^7} \cdot (n_{p,f} + \bar{n}_{p,f}) \\
& + \frac{3p^4 M^2}{4TE_p^6} \cdot \left(\frac{1}{\cosh^2(\frac{E_p+\mu}{2T})} + \frac{1}{\cosh^2(\frac{E_p-\mu}{2T})} \right) \\
& + \frac{k^2 \cdot (E_p^2 - 2M^2)}{2T \cdot E_p^4} \cdot \left(\frac{1}{\cosh^2(\frac{E_p+\mu}{2T})} + \frac{1}{\cosh^2(\frac{E_p-\mu}{2T})} \right) \\
& + \frac{p^2 M^2}{2T^2 \cdot E_p^3} \cdot \left(\frac{\tanh(\frac{E_p+\mu}{2T})}{\cosh^2(\frac{E_p+\mu}{2T})} + \frac{\tanh(\frac{E_p-\mu}{2T})}{\cosh^2(\frac{E_p-\mu}{2T})} \right) \\
& - \frac{p^2}{2T} \cdot \left(\frac{3M^2 E_p^2 - 4 \cdot M^4}{E_p^6} \cdot \left(\frac{1}{\cosh^2(\frac{E_p+\mu}{2T})} + \frac{1}{\cosh^2(\frac{E_p-\mu}{2T})} \right) \right) \\
& - \frac{p^2 M^4}{2T^2 E_p^5} \cdot \left(\frac{\tanh(\frac{E_p+\mu}{2T})}{\cosh^2(\frac{E_p+\mu}{2T})} + \frac{\tanh(\frac{E_p-\mu}{2T})}{\cosh^2(\frac{E_p-\mu}{2T})} \right) \\
& - \frac{3p^2 (M^2 E_p^2 - M^4)}{4T^2 E_p^5} \cdot \left(\frac{\tanh(\frac{E_p+\mu}{2T})}{\cosh^2(\frac{E_p+\mu}{2T})} + \frac{\tanh(\frac{E_p-\mu}{2T})}{\cosh^2(\frac{E_p-\mu}{2T})} \right) \\
& \left. - \frac{p^2 M^4}{8T^3 E_p^4} \cdot \left(\frac{\cosh^2(\frac{E_p+\mu}{2T}) - 3 \cdot \sinh^2(\frac{E_p+\mu}{2T})}{\cosh^4(\frac{E_p+\mu}{2T})} + \frac{\cosh^2(\frac{E_p-\mu}{2T}) - 3 \cdot \sinh^2(\frac{E_p-\mu}{2T})}{\cosh^4(\frac{E_p-\mu}{2T})} \right) \right] \tag{A.6}
\end{aligned}$$

The forth derivative at the point $M = 0$

$$\frac{\partial^4 \Omega_0(T, \mu; M)}{\partial M^4} \Big|_{M=0} = -\frac{3}{\pi^2} \left[3 - \int_0^\Lambda dp \frac{3}{p} + \int_0^\infty dp \frac{3}{p} (n_{p,f} + \bar{n}_{p,f}) \right] \tag{A.7}$$

Literaturverzeichnis

- [1] G. Ecker: *Quantum Chromodynamics*, Lectures given at the 2005 European School of High-Energy Physics, 2006, arXiv:hep-ph/0604165
- [2] M. Durante et al.: *All the Fun of the FAIR: Fundamental physics at the Facility for Antiproton and Ion Research*, Physica Scripta 94, 033001, 2019, arXiv:1903.05693.
- [3] Y. Nambu, G. Jona-Lasinio: *Dynamical Model of Elementary Particles Based on an Analogy with Superconductivity. I.*, Phys. Rev. 122, 345-358, 1961
- [4] Y. Nambu, G. Jona-Lasinio: *Dynamical Model of Elementary Particles Based on an Analogy with Superconductivity. II.*, Phys. Rev. 124, 246-254, 1961
- [5] M. Asakawa and K. Yazaki, Nucl. Phys. A 504 (1989) 668.
- [6] S.P. Klevansky, Rev. Mod. Phys. 64 (1992) 3.
- [7] M. Buballa: *NJL-model analysis of dense quark matter*, Phys. Rep. 407, 205-376, 2005, arXiv:hep-ph/0402234v2
- [8] M. Frank, (2003). *Das QCD-Phasendiagramm bei endlicher Isospindichte*, (Diplom thesis). TU Darmstadt, Darmstadt, Deutschland.
- [9] F. Schwabel: *Statistische Mechanik*, 3rd edition, Springer-Verlag, Heidelberg, 2006
- [10] M. Frank, M. Buballa, M. Oertel: *Flavor-Mixing Effects on the QCD Phase Diagram at non-vanishing Isospin Chemical Potential: One or Two Phase Transitions?*, Phys.Lett. B562 (2003) 221-226, 2003, arXiv:hep-ph/0303109

Erklärung zur Abschlussarbeit gemäß §22 Abs. 7 und §23 Abs. 7 APB der TU Darmstadt

Hiermit versichere ich, Dominik Erb, die vorliegende Bachelorarbeit ohne Hilfe Dritter und nur mit den angegebenen Quellen und Hilfsmitteln angefertigt zu haben. Alle Stellen, die Quellen entnommen wurden, sind als solche kenntlich gemacht worden. Diese Arbeit hat in gleicher oder ähnlicher Form noch keiner Prüfungsbehörde vorgelegen.

Mir ist bekannt, dass im Fall eines Plagiats (§38 Abs. 2 APB) ein Täuschungsversuch vorliegt, der dazu führt, dass die Arbeit mit 5,0 bewertet und damit ein Prüfungsversuch verbraucht wird. Abschlussarbeiten dürfen nur einmal wiederholt werden.

Bei der abgegebenen Thesis stimmen die schriftliche und die zur Archivierung eingereichte elektronische Fassung gemäß §23 Abs. 7 APB überein.

Bei einer Thesis des Fachbereichs Architektur entspricht die eingereichte elektronische Fassung dem vorgestellten Modell und den vorgelegten Plänen.

Darmstadt, 26. Januar 2020

Dominik Erb